IEEE Access
Multidisciplinary ⋮ Rapid Review ⋮ Open Access Journal

Received November 3, 2019, accepted November 20, 2019, date of publication December 2, 2019,
date of current version December 23, 2019.

Digital Object Identifier 10.1109/ACCESS.2019.2957126

Design, Modeling and Experimental Validation of a Variable Resonant Electro-Hydraulic Fatigue Testing System

YAN REN[1], JIPING BAI[2], AND JIAN RUAN[3]

[1]College of Mechanical and Electrical Engineering, Wenzhou University, Wenzhou 325035, China
[2]Rail Transit Department, Zhejiang Institute of Communications, Hangzhou 311112, China
[3]Key Laboratory of Special Purpose Equipment and Advanced Machining Technology, Ministry of Education, Zhejiang University of Technology, Hangzhou 310014, China

Corresponding author: Jian Ruan (yanyan333@126.com)

This work was supported in part by the National Natural Science Foundation of China under Grant 51805376 and Grant U1709208, in part by the Zhejiang Provincial Natural Science Foundation of China under Grant LY20E050028, in part by the Special Equipment Manufacturing and Advanced Processing Technology, Ministry of Education, Zhejiang Provincial Key Laboratory Open Fund Project, under Grant EM2018120103, and in part by the Wenzhou Basic Scientific Research Foundation of China under Grant G20180021.

ABSTRACT High frequency excitation in the electro-hydraulic mode, especially kilohertz regime, has already been realized owing to the merits of specially designed two-dimensional rotary valve (2D rotary valve). However, some sacrifice in the excitation amplitude is inevitable as pursuing the higher excitation frequency. A scheme for an electro-hydraulic excitation system working at resonant is proposed, which could accomplish high excitation frequency and large vibration amplitude simultaneously. More specifically, the resonant frequency of this system can be regulated as loads of the excitation system, which would greatly facilitate fatigue testing of different elastomeric materials. This paper investigates more details of the excitation characteristics in whole frequency domain, including non-resonance and variable resonance. The excitation waveforms, variable resonant frequency and resonant peak are derived and validated by experimental data. This work provides clear analytical expressions of the mathematical model, offers important guidance for the design of the system, and paves the way for the potential engineering application of the variable resonant excitation technology.

INDEX TERMS Rotary valve, electro-hydraulic type variable resonant excitation, analytical expressions, hydraulic resonance.

I. INTRODUCTION

High frequency excitation techniques, including electrodynamics, electromagnetic or ultrasonic modes, generally have the drawback of the small excitation force [1]–[3]. In contrast, the electro-hydraulic excitation mode is characterized by the large excitation force, but increasing the excitation frequency up to the kilohertz-level is not easy [4], [5].

Many researches on the realizing high frequency excitation have been developed [6], [7]. In these schemes, the electro-hydraulic excitation system driven by the rotary valve, instead of the conventional sliding valve, is considered to be a novel technology for significantly improving the excitation frequency. Inspired by the swing structure of the vibrator that induces the high frequency excitation [8], Zhao et al. designed a revolving valve, in which a rotating spool is utilized to distribute the flow rate [9]. This valve was theoretically designed to be used in a hydraulic vibratory hammer to achieve higher vibration frequencies, or even stepless frequency regulation. Some other researchers have done some preliminary researches on new rotary valve prototypes [10], [11]. Li et al. proposed a new three-way on/off valve to generate high frequency discrete flow, which was used in a virtually variable displacement pump system. The frequency of this switch could reach 100 Hz by the rotary motion of the spool [12]. Pournazeri et al. proposed a pressure-driven rotary valve to control the inlet or discharge flow in a lift control mechanism [13]. The rotary speed of this valve was proportional to the engine speed, which was analogous to the proportional valve function. Similar to the speed and

The associate editor coordinating the review of this manuscript and approving it for publication was Jianyong Yao.

angular position controlled independently, the rotary and sliding motion of a single spool in a new rotary were also controlled separately. In this sense, it was referred to as a 2D rotary valve. This rotary valve was presented by Ruan [14], of which the novel architecture is easily to realize the oil flow reversing quickly. So it is very suitable to be employed in exciting systems. Xing et al. developed a flutter device is equipped with this 2D rotary valve, which significantly extended the excitation frequency beyond the system resonant frequency [15].

Although high excitation frequency could be increased, in most excitation systems, trade-off of the excitation amplitude is inevitable. Some researches about increasing the excitation amplitude at high excitation frequencies have been developed. For instance, a traditional 250 kN frame was redesigned by MTS Systems Corporation, which enabled higher actuator displacements at a frequency of 1000 Hz [16]. It was generally used in a servo hydraulic system for elastomeric material fatigue testing and crack growth testing. In addition, some control compensation strategies were designed and applied [17]–[19]. Three-variable-controller was widely applied in the electro-hydraulic vibration system to track amplitude, velocity or acceleration of the vibration in a closed loop mode [20]–[22]. Plummer [23] and Wei *et al.* [24] did some work about improving the stability of the output vibration including the vibration amplitude. Shen et al. proposed a hybrid control strategy, forward feed compensation method combined with adaptive inverse control algorithm, in order to adjust the vibration amplitude [25].

In addition to the trade-off between the excitation amplitude and the frequency, the electro-hydraulic excitation mode is very time-consuming and extremely expensive because of the high electrical power required by the hydraulic pumps used for the hydraulic oil supply. As a result, performing the test especially a great many cycles within a relatively short time period has become critical for enormously reducing energy costs. Therefore, a resonant type of excitation system is required [26]. There have been several researches about resonant testing or testing system. For example, resonant testing facilities were developed in order to induce fatigue failure in the specimen [27]. However, these researches mainly focused on electrodynamics or electromagnetic excitation mode [28], [29], because high frequency operation of the electro-hydraulic excitation system itself remains a challenge.

In this direction, this paper proposes a novel resonant electro-hydraulic fatigue testing system, which creates a forced excitation close to the natural frequency of the hydraulic system in order to utilize the excitation at resonant frequency. The aim of the project is to accomplish high excitation frequency and large vibration amplitude simultaneously. More specifically, the resonant frequency of this system can be regulated as loads of the excitation system, which would greatly facilitate fatigue testing of different elastomeric materials. The novel proposed technology provides 10^9 high cycle testing with resonant frequencies at min. 720 Hz and max. 924 Hz, while a conventional hydraulic fatigue testing time is limited up to 10^6-10^7 cycles owing to the lower frequency range of approximately 2-300 Hz. Besides the advantage of reducing the test duration, dramatic reduction in electrical energy consumption was achieved. In the following texts, the structure design, the mathematical models including non-resonance and resonance, and the preliminary testing results of the variable resonant excitation system are presented.

II. A VARIABLE RESONANT ELECTRO-HYDRAULIC FATIGUE TESTING SYSTEM

Fig.1 shows the schematic diagram of the proposed variable resonant electro-hydraulic fatigue testing system, which mainly consists of the 2D rotary valve, hydraulic cylinder, bias servovalve, clamping fixture and rigid frame. Three-way rotary valve must be used with an unequal area piston in the hydraulic cylinder to provide direction reversal. When the fluid through valve ports (meter-in) flows into the head chamber, the piston is pushed up. While the spool rotates an angle, the fluid through valve ports (meter-out) flows out of the head chamber, the piston is down. This is an ordinary combination of a three-way valve and a single-rod cylinder, but the special is that rotating motion of the spool (not sliding motion) corresponding valve structure is applied to distribute oil. In this 2D valve, the single spool has two degrees of freedom including rotational and sliding motion. The excitation frequency is proportional to the rotary speed of the spool. The rotary spool is lubricated using oil, therefore, it is easily to achieve high excitation frequencies through increasing the rotary speed of the spool. Owing to the merits of 2D rotary valve, the system can operate at resonance. And the excitation cylinder as the piston actuator with single rod combined with the rotary valve is specially designed in order to regulate the natural frequency of this system, although the adjustable

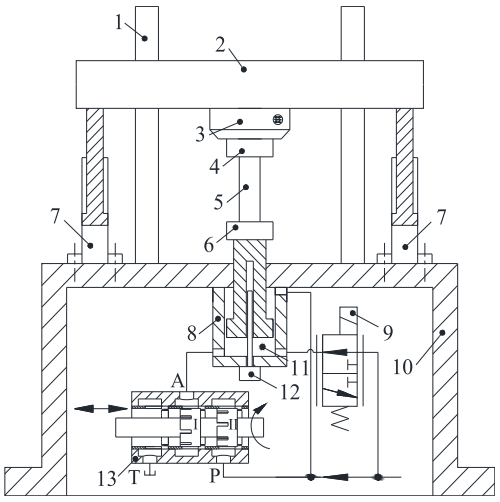

FIGURE 1. Variable resonant electro-hydraulic fatigue testing system. 1-box column; 2-beam; 3-force cell; 4-upper gripper head; 5-specimen; 6-lower gripper head; 7-synchronic hydrocylinder; 8-excitation cylinder; 9-servovalve; 10-base; 11-head chamber; 12-displacement transducer; 13-2D rotary valve.

range is limited. The initial volume of the head chamber of the cylinder, is controlled by the bias servovalve paralleled with 2D rotary valve. These key components control the flow of oil and transform the motion of the flow into the oscillation of the piston including operate at resonance.

The clamping fixture of the fatigue testing system mainly includes gripper heads, the beam and a synchronizing device. The test sample (the specimen) is held by two gripper heads, the upper gripper head is regulated by synchronic hydrocylinders, while the lower one is connected to the piston of the cylinder. As a result, the oscillating excitation is conveyed to the test sample. Magnitude of the excitation force is measured by a force cell, which is placed between the upper gripper head and the beam. The excitation waveform (especially low frequency waveform) is measured by a displacement transducer mounted inside the piston rod of the cylinder.

Although the proposed electro-hydraulic fatigue testing system is the combination of a valve and piston as frequently seen in other hydraulic power system, it can operate at different resonant frequencies. And the hydraulic natural frequency varies with the volume of the head chamber, which strongly depends on the loads. Therefore, the variable resonant frequency is a characteristic indicator of the load of this electro-hydraulic exciter. As a result, an application of this technique in resonant fatigue tests of different elastomeric materials is, in principle, a scheme of potential success.

III. MECHANISM OF 2D ROTARY VALVE

Three-way valve-piston combinations, as power elements usually in hydromechanical position servos [30], is applied here in electro-hydraulic fatigue testing system which performs inducing fatigue failure of the specimen at different resonant frequencies. In the combination, the three-way 2D rotary valve instead of the four-way has been redesigned as shown in Fig.2. The spool has just two shoulders, more grooves are evenly distributed on every shoulder. Moreover, drive mode of the spool and corresponding structure for realizing the function of the driving are improved. The rotational motion of the spool is actuated by a servo motor connected to a geared assembly. The geared arrangement with a gear ratio of 1:4 is designed to amplify the motor speeds proportionally in order to increase the rotary speed of the spool. The axial sliding is directly controlled by a linear stepping motor through the connected bulkhead and the spring in the other end of the spool. Instead of the former complicated eccentric mechanism, this axial displacement control is more accurate.

The sectional views of the shoulder and sleeve are shown in Fig.3. There are sixteen grooves are on the circumference of the shoulder (if the central angle of the groove is α, the central angle between two adjacent grooves on one shoulder is defined as 4α). Correspondingly, an equal number of T-slot windows are evenly distributed on a circle of the sleeve. For a T-slot window, the narrow, horizontal part along the axis of the spool is to match the groove to form the throttling orifice, while the wide, circumferential part is specially designed for

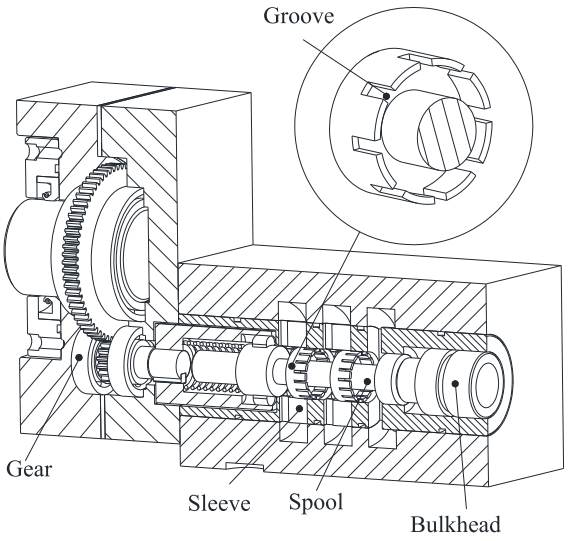

FIGURE 2. Three-way 2D rotary valve concept.

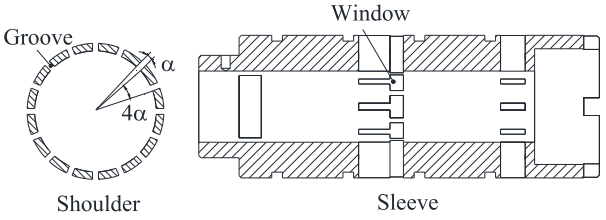

FIGURE 3. Sectional view of the shoulder and sleeve.

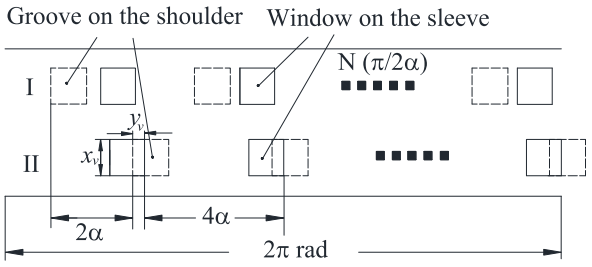

FIGURE 4. Geometry of the groove and window.

dissipating the congested fluid and ensure the flowing steady-state without rotary speed sacrifice. As the continuous rotary of the spool, grooves on the shoulder of the spool matched the windows on the sleeve form the throttling orifices. Similar to the working principle of the three-way slide valve, the meter-in ports of one shoulder and meter-out ports of another shoulder are alternately active.

Rectangular valve orifices are formed as grooves on the shoulder of the spool and windows on the sleeve overlap with each other. The length of one side of the orifices is the peripheral width of the groove overlapped by the window, while the length of the lateral side is determined by spool's axial position, as shown in Fig.4. It is noteworthy that grooves on adjacent shoulders have an angle difference of 2α between them. Such a configuration creates an 'alternately varied' valve port area, that is, either shoulder I or II is active.

With reference to Fig.4, if the number of grooves on a single shoulder (or corresponding windows on the sleeve) is N, N valve orifices (formed by grooves and windows) will open or close simultaneously and work in exactly the same process as the spool rotates in one cycle. In this scenario, the excitation frequency of the system is N times the rotary frequency of the spool. Therefore, high excitation frequency can be easily achieved by not only increasing the rotary speed of the spool, but also increasing the number of grooves/windows reasonably. Although more grooves/windows is more advantageous to increase the excitation frequency of the system in theory, determining the number of grooves/windows actually depends on many factors, e.g. the processing problem should be considered, as well as the flow rate should be satisfied (it is related to the size of the valve port).

There is a coupling relation between oscillating frequency and excitation force. Therefore, compromise of the excitation amplitude is inevitable in achieving high frequency, although in the rotary controlled system the excitation amplitude could be improved independently within a small range through adjusting the axial displacement of the spool.

IV. DESIGN AND MODELING ANALYSIS

A design and analysis equations of the variable resonant electro-hydraulic exciter are presented in this section. For the theoretical analysis, several assumptions are made: (1) The 2D rotary valve has perfect geometry with orifices matched symmetrically. (2) The amplitude of piston motion is significantly smaller than the length of the head chamber. (3) The friction is neglected. (The system pressure required to counteract the frictional force of rationally designed hydraulic cylinder is usually less than 0.3 MPa, which is negligible considering that practical system pressure that usually runs above 21 MPa). (4) The leakage of piston is neglected.

A. BASIC EQUATION

The flow equation of the valve orifice is written as

$$Q_L = \begin{cases} C_d A_{11}(\theta)\sqrt{\dfrac{2\,(p_s - p_c)}{\rho}} & 0 \le \theta < 2\alpha \\ -C_d A_2(\theta)\sqrt{\dfrac{2p_c}{\rho}} & 2\alpha \le \theta < 4\alpha \end{cases} \tag{1}$$

where Q_L is the flow rate through the 2D rotary valve orifices, C_d is the discharge coefficient, $A_{vi}(\theta)$ is instantaneous orifice areas on shoulder i ($i = 1, 2$ for shoulder I and II respectively) of the spool, θ is the the rotation angle, ρ is density of oil, p_c is control pressure in head chamber, p_s is the system pressure. When the spool rotates at a constant angular frequency ω_v, $\theta = \omega_v t$.

The instantaneous orifice areas (formed by grooves and windows) are

$$A_{v1}(\theta) = z x_v y_v = \begin{cases} 2z_v r \sin\left(\dfrac{\theta}{2}\right) & 0 \le \theta < \alpha \\ 2z_v r \sin\left(\alpha - \dfrac{\theta}{2}\right) & \alpha \le \theta < 2\alpha \\ 0 & 2\alpha \le \theta < 3\alpha \\ 0 & 3\alpha \le \theta < 4\alpha \end{cases} \tag{2}$$

$$A_{12}(\theta) = z x_v y_v = \begin{cases} 0 & 0 \le \theta < \alpha \\ 0 & \alpha \le \theta < 2\alpha \\ 2z_v r \sin\left(\dfrac{\theta}{2} - \alpha\right) & 2\alpha \le \theta < 3\alpha \\ 2z x_v \sin\left(2\alpha - \dfrac{\theta}{2}\right) & 3\alpha \le \theta < 4\alpha \end{cases} \tag{3}$$

where z is the number of grooves/windows, x_v is axial displacement of spool, y_v is the section where the groove overlaps with the window, r is radius of the spool.

Here, y_v is actually a circular arc, so orifice areas are rewritten as

$$A_{11}(\theta) = z x_v y_v = \begin{cases} z x_v r\theta & 0 \le \theta < \alpha \\ 2z x_v r\alpha - z x_v r\theta & \alpha \le \theta < 2\alpha \\ 0 & 2\alpha \le \theta < 3\alpha \\ 0 & 3\alpha \le \theta < 4\alpha \end{cases} \tag{4}$$

$$A_{v2}(\theta) = z x_v y_v = \begin{cases} 0 & 0 \le \theta < \alpha \\ 0 & \alpha \le \theta < 2\alpha \\ -2z x_v r\alpha + z x_v r\theta & 2\alpha \le \theta < 3\alpha \\ 4z x_v r\alpha - z x_v r\theta & 3\alpha \le \theta < 4\alpha \end{cases} \tag{5}$$

Application of the continuity equation to the control chamber yields

$$Q_L = \frac{A_h dy_p}{dt} + \frac{V_0 dp_c}{E_h dt} \tag{6}$$

where A_h is the head side area, y_p is the excitation displacement, V_0 is the initial head chamber volume, E_h is the effective bulk modulus.

The resulting force equation is

$$p_c A_h - p_s A_v = m\frac{d^2 y_p}{dt^2} + B_p \frac{dy_p}{dt} + K_L y_p + F_L \tag{7}$$

where $A_h = 2A_r$ is rod side area of the piston, m is total mass of piston together with the load referred to piston, B_p is viscous damping coefficient, K_L is load spring gradient, F_L is a constant or arbitrary force.

B. EXCITATION WAVEFORMS

Each of the usual loads (mass, viscous, and spring forces) impacting on the specimen varies in different excitation frequency domains. For different loads, three describing functions of excitation waveforms are distinguished, with their respective applications in different circumstances.

1) LOW FREQUENCY DOMAIN

Low frequency refers to the frequency which is far below the system natural frequency. In this frequency domain, the force required for acceleration during a vibration cycle is small compared with that required for displacement dependent terms. Therefore, the dominance of spring load is assumed, the force equation for piston is rewritten as

$$p_c A_h - p_s A_r = K_L y_p \tag{8}$$

Assuming that the excitation is a persistent amplitude vibration, with the amplitude [10], A_{fl}, being

$$A_{fl} = \frac{A_r}{K_L}\sqrt{p_s^2 - \left[p_s - \frac{1}{2}\left(\frac{C_0 K_L z x_v r \alpha^2}{2\omega_v A_r}\right)^2\right]^2} \tag{9}$$

where $C_0 = C_d \Big/ \left[\sqrt{\rho}\left(A_h + \frac{V_0 K_L}{E_h A_h}\right)\right]$

It is noteworthy that 'pressure saturation' may occur in the low-frequency domain. The pressure inside the head chamber increases very rapidly and then reaches the system's pressure, although the orifice area is very small in magnitude. In a result, there is no flow rate (it drops down to zero) through the valve port flowing into or out of the system during the 'pressure saturation'. Consequently, the output displacement reaches the extreme value, $p_s A_r / K_L$. In this case, the position of rotary spool of the valve (displays a knee) is

$$\theta' = \begin{cases} \sqrt{\dfrac{4\omega_v A_v \sqrt{2p_s}}{C_0 K_L z x_v}} & 0 \le \theta' < \alpha \\ \sqrt{\dfrac{4\omega_v A_r \sqrt{2p_s}}{C_0 K_L z x_v r}} + 2\alpha & 2\alpha \le \theta' < 3\alpha \end{cases} \tag{10}$$

$$\theta'' = \begin{cases} 2\alpha - \sqrt{2\alpha^2 - \dfrac{4\omega_e A_{\sqrt{2}} \sqrt{2p_s}}{C_0 K_L z x_v}} & \alpha \le \theta'' < 2\alpha \\ 4\alpha - \sqrt{2\alpha^2 - \dfrac{4\omega_v A_v \sqrt{2p_s}}{C_0 K_L z x_v r}} & 3\alpha \le \theta'' < 4\alpha \end{cases} \tag{11}$$

It is difficult to maintain the excitation amplitude at a high level when the excitation frequency is increased. As a result, the pressure saturation or displacement saturation rarely takes place in other higher frequency bands.

2) MID FREQUENCY DOMAIN

Mid frequency band is one particular case in which the excitation frequency is lower than that in the high frequency domain, while higher than that in the low frequency domain. Its output amplitude is very small, just compared with that of lower frequency domain. Under such conditions, inertia force and spring force may be entirely neglected. Thus, the electro-hydraulic exciter can be considered to be an ideal system without load. The force equation for piston is rewritten as

$$p_c A_h - p_s A_r = 0 \tag{12}$$

(1), (6) and (12) are three basic equations and may be solved simultaneously as

$$\frac{C_1 A}{\omega_v} d\theta = dy_p \tag{13}$$

where $C_1 = C_d \sqrt{P_s / \rho / A_h}$

Substituting (4) and (5) into (13) and the output displacement is

$$y_p = \begin{cases} y_i + \dfrac{C_1 z x_i \cdot \theta^2}{2\omega_v} & 0 \le \theta < \alpha \\ y_i + \dfrac{C_1 z x_i}{\omega_v}\left(2\alpha\theta - \dfrac{\theta^2}{2} - \alpha^2\right) & \alpha \le \theta < 2\alpha \\ y_r + \dfrac{C_1 z x_i}{\omega_v}\left(2\alpha\theta - \dfrac{\theta^2}{2} - 2\alpha^2\right) & 2\alpha \le \theta < 3\alpha \\ y_r + \dfrac{C_1 z x_i}{\omega_v}\left(-4\alpha\theta + \dfrac{\theta^2}{2} + 7\alpha^2\right) & 3\alpha \le \theta < 4\alpha \end{cases} \tag{14}$$

where y_r and y_l are the positive and negative end position of the excitation, respectively, if the central position of the vibration is assumed to be zero.

The amplitude, A_{fm}, is

$$A_{fm} = y_r = -y_l = \frac{C_1 z x_v r \alpha^2}{2\omega_v} \tag{15}$$

3) HIGH FREQUENCY DOMAIN

High frequency band is close to the system natural frequency. In this case, the acceleration of piston is so conspicuously high that the driving force is consumed mainly by mass load. The force equation for piston can be approximated as

$$p_c A_h - p_s A_r = m\frac{d^2 y_p}{d^2 t} \tag{16}$$

Assuming that the output excitation waveform is

$$y_p = A_{fh} \sin\left(\omega_p t - \pi/2\right) \tag{17}$$

where A_{fh} is the amplitude of the excitation waveform, ω_p is the working frequency of the testing system, which is relative to ω_v, $\omega_p = \omega_v$.

Substituting (17) into (16) yields

$$P_c A_h - P_i A_r = -m\omega_p^2 y_p \tag{18}$$

Compared with (8), (18) implies that the load is analogous to the spring load, although the 'spring stiffness' ($p_c A_h - p_s A_r = -m\omega_p^2 y_p$) is a negative value different from ordinary situation. Referring to (18), the ''spring'' is in its natural state as the pressure in the control chamber is a half of the system pressure. This is also the central position of the excitation, $y_p = 0$.

(1), (6) and (18) can be solved simultaneously as

$$\frac{C_2 A_{v1}(\theta)}{\omega_v} d\theta = \frac{1}{\sqrt{p_s + m\omega_p^2 y_p \Big/ A_r}} dy_p \quad (0 \le \theta < 2\alpha) \tag{19}$$

$$\frac{-C_2A_{v2}(\theta)}{\omega_v}d\theta = \frac{1}{\sqrt{p_s - m\omega_p^2 y_p / A_r}}dy_p \quad (2\alpha \le \theta < 4\alpha) \tag{20}$$

where $C_2 = C_d \Big/ \left[\sqrt{\rho}\left(A_h - \frac{m\omega_p^2 V_0}{E_h A_h}\right)\right]$

Substituting (4) and (5) into (20) and (21), the output displacement in high frequency domain is obtained as

$$Y_p = y_p / y_u = \begin{cases} p_s^{-1}\left[p_s - \left(\sqrt{p_s + \frac{m\omega_p^2 y_l}{A_r}} + \frac{C_2 z x_v r m\omega_p^2 \theta^2}{4\omega_v A_r}\right)^2\right] & 0 \le \theta < \alpha \\ p_s^{-1}\left\{p_s - \left[\sqrt{p_s + \frac{m\omega_p^2 y_l}{A_r}} + \frac{C_2 z x_v r m\omega_p^2}{2\omega_v A_r} \times \left(2\alpha\theta - \frac{\theta^2}{2} - \alpha^2\right)\right]^2\right\} & \alpha \le \theta < 2\alpha \\ -p_s^{-1}\left\{p_s - \left[\sqrt{p_s - \frac{m\omega_p^2 y_r}{A_r}} - \frac{C_2 z x_v r m\omega_p^2}{2\omega_v A_r} \times \left(2\alpha\theta - \frac{\theta^2}{2} - 2\alpha^2\right)\right]^2\right\} & 2\alpha \le \theta < 3\alpha \\ -p_s^{-1}\left\{p_s - \left[\sqrt{p_s - \frac{m\omega_p^2 y_r}{A_r}} - \frac{C_2 z x_v r m\omega_p^2}{2\omega_v A_r} \times \left(\frac{\theta^2}{2} - 4\alpha\theta + 7\alpha^2\right)\right]^2\right\} & 3\alpha \le \theta < 4\alpha \end{cases} \tag{21}$$

where y_u is an extreme value when the control pressure in the head chamber reaches the system pressure, *i. e.*, $y_u = p_s A_r / K_L$.

Amplitude of vibration can be described by

$$A_{fh} = y_r = -y_l = \frac{A_r}{m\omega_p^2}\sqrt{p_s^2 - \left[p_s - \frac{1}{2}\left(\frac{C_2 z x_v r m\omega_p^2 \alpha^2}{2\omega_v A_r}\right)^2\right]^2} \tag{22}$$

Referring to (22), the excitation amplitude decreases steeply as the excitation frequency is increased.

V. HYDRAULIC RESONANCE

With reference to Fig.5, the fluid flows into the head chamber of the hydraulic cylinder as ports on the shoulder I are active. However, different from the traditional, the piston keeps moving forwards (the head chamber) off the central position of the excitation (depicted by the dotted line) with a certain velocity, as shown in state ①. At the central position,

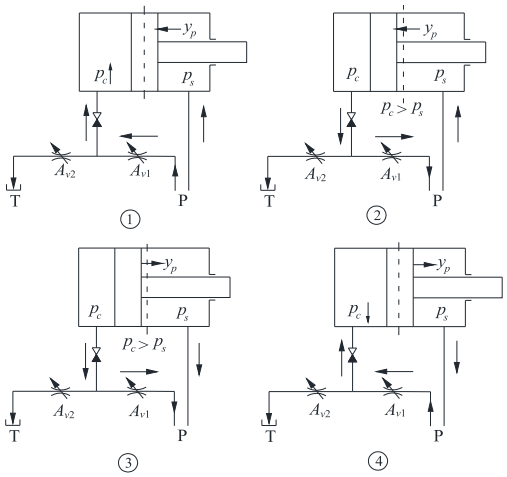

FIGURE 5. Hydraulic resonance in the head chamber (shoulder I is active).

the system has the maximum kinetic energy with the effect of inertia dominating its behavior. As the piston is continuous to move forwards, the fluid in the head chamber is compressed, in a result the pressure there increases rapidly, kinetic energy of the fluid is converted into potential energy and stored in the fluid spring until the piston stops. At this state, the pressure of the compressed fluid is reaches a maximum value beyond the system pressure, which causes the fluid flowing back to the ports, as shown in state ②. The high pressure in the head chamber pushes the piston back to the central position and the potential energy of the fluid is again converted into kinetic energy, as shown in state ③. As the piston moves backwards, the increasing volume of the head chamber relieves the pressure of holding in the head chamber. Once the pressure in the head chamber decreases below the system pressure, the fluid begins to flow into the head chamber, the piston thereby rapidly moves rightwards, as shown in the state ④.

The process of hydraulic motion in the rightwards is similar to that in the leftwards. The piston keeps moving rightwards after passing the central position under the effect of inertia. At this time, the fluid flows out from the head chamber as ports on the shoulders II are active. The pressure in the head chamber keeps decreasing until the lowest pressure is reached (when the pressure decreases below the atmospheric pressure, the oil will be drawn from the tank into the head chamber), during which kinetic energy decreases to zero. Afterwards, the potential energy of the fluid is released and the piston moves back to the central position, as shown in the state ⑤ to ⑧ in Fig.6.

It is obvious that the main mechanism of the periodic motion of the piston in the above mentioned system is the conversion between kinetic and potential energies.

A. OVERALL NATURAL FREQUENCY

A block diagram of the excitation system is formed in Fig.7. It contains two parts, nonlinear and linear. The nonlinear part, including the pressure-flow relationship of the valve port,

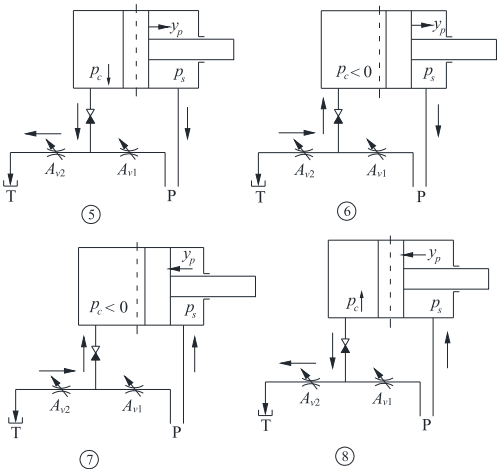

FIGURE 6. Hydraulic resonance in the head chamber (shoulder II is active).

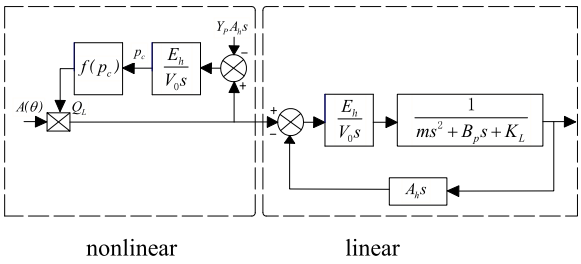

FIGURE 7. The block diagram of the testing system model.

has been separated from a quadratic linear part with the piston displacement feedback.

The transfer function for the linear region is

$$\frac{Y_p}{Q_L} = \frac{\frac{E_h A_h}{V_0 K_L + E_h A_h^2}}{s[\frac{s^2}{(V_0 K_L + E_h A_h^2)/(V_0 m)} + \frac{s}{(V_0 K_L + E_h A_h^2)/(V_0 B_p)} + 1]} = \frac{K_V}{s(\frac{s^2}{\omega_0^2} + \frac{2\delta_0 s}{\omega_0} + 1)} \tag{23}$$

where K_v is the flow gain, ω_0 is over-all natural frequency, δ_0 is damping ratio (dimensionless).

Referring to Eq. (23), the expression of the over-all natural frequency is

$$\omega_0 = \sqrt{\frac{V_0 K_L + E_h A_h^2}{V_0 m}} = \sqrt{\omega_h^2 + \omega_m^2} \tag{24}$$

where ω_h is the undamped hydraulic natural frequency, $\omega_h = \sqrt{E_h A_h^2 / (V_0 m)}$, ω_m is the structural natural frequency, $\omega_m = \sqrt{K_L / m}$.

The over-all natural frequency, ω_0, consists of two parts, a fluid spring part with a hydraulic spring rate $E_h A_h^2 / V_0$ and a mechanical part with a load spring constant of K_L. Interaction of the spring effect of a liquid and the mass of mechanical parts gives the over-all natural frequency. It implies that the volume of the initial head chamber (V_0) is adjustable (it could be controlled by a servo valve), contributing to a variable hydraulic resonant frequency.

B. RESONANT PEAK

At resonance, the excitation displacement has a phase angle difference of 90° compared with the non-resonant waveforms. Assuming that the resonant waveform consists of the fundamental frequency only, it could be expressed as

$$y_{rp}(\theta) = A_{rf} \sin(z\theta - \pi) \quad 0 \le \theta \le 4\alpha \tag{25}$$

where $y_{rp}(\theta)$ is the resonant displacement, A_{rf} is the resonant peak of the displacement waveform.

The pressure in the head chamber, $p_{rc}(\theta)$, is

$$p_{rc}(\theta) = p_{rL\max} \sin(z\theta) + \frac{1}{2} p_s \tag{26}$$

where $p_{rL\max}$ is the amplitude of the pressure drop across the load at resonance.

The flow through the load at resonance is

$$Q_{rL}(\theta) = \begin{cases} \text{sign}[p_s - p_{rc}(\theta)] C_d A_{v1}(\theta) \sqrt{\frac{2|p_s - p_{rc}(\theta)|}{\rho}} \\ \quad \theta \in [0, 2\alpha) \\ \text{sign}[p_{rc}(\theta)] C_d A_{v2}(\theta) \sqrt{\frac{2|p_{rc}(\theta)|}{\rho}} \\ \quad \theta \in [2\alpha, 4\alpha) \end{cases} \tag{27}$$

Assuming that the hydraulic horsepower is completely converted into work done by the piston, the conservation of energy requires that

$$\int_0^{4\alpha} p_{rL}(\theta) Q_{rL}(\theta) d\theta = 0 \tag{28}$$

where $p_{rL}(\theta)$ is the load pressure, $p_{rL}(\theta) = p_{rc}(\theta) - p_s/2$.

Equations (26), (27) and (28) can be solved simultaneously using the Runge-Kutta method, the pressure peak at resonance is obtained numerically as

$$p_{rc\max} = (w + 0.5) p_s \tag{29}$$

where w is a pressure ratio, $0.5 < w < 0.6$.

These general equations are used to derive the pressure-flow curve, as shown in Fig.8.

As shown in Fig.8, the pressure peak may become higher than the system pressure. At this state, the fluid flows in the reverse direction, which avoids continuous increase of resonant peak and potential damage to the hydraulic system. It is evident that the hydraulic actuator (the hydraulic cylinder) acts as a power element, i. e., processes ② and ③ are analogous to the delivery of oil of pumping actions, while ⑥ and ⑦ are similar to the oil suction. Therefore, energy could be saved if the excitation is performed at resonance.

Assuming that the force equation of the piston is

$$p_{rc}(\theta) A_h - p_s A_r = m \frac{d^2 y_{rp}(\theta)}{d^2 t} + K_L y_{rp}(\theta) \tag{30}$$

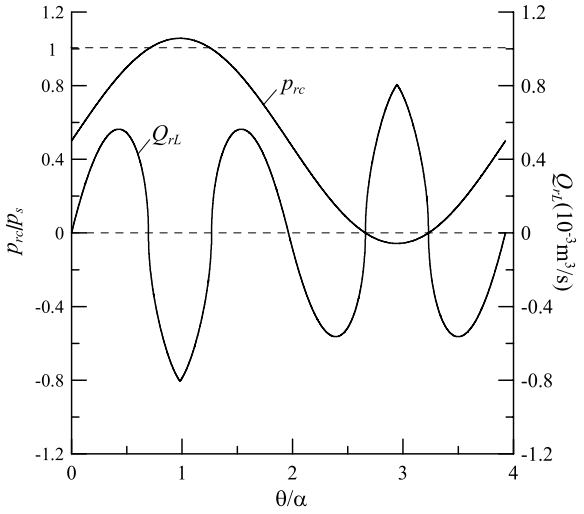

FIGURE 8. Pressure-flow curve for the variable resonant exciter.

Substituting (25), (26) into (30), the resonant peak is obtained as

$$A_{rf} = \frac{p_{rL\max} V_0}{E_h A_h} \tag{31}$$

From this expression, we know that the resonant peak is approximately a constant that depends on system parameters, but is independent of the opening areas of valve ports.

VI. EXPERIMENTS AND RESULTS

A. EXPERIMENTAL HARDWARE

The prototype of the variable resonant electro-hydraulic fatigue testing system is shown in Fig.9. The system has been integrated for high frequency fatigue testing in Zhejiang University of Technology, as shown in Fig.9 (a). The 2D rotary valve and the bias servovalve are in Fig.9 (b) and (c). The system had successfully accomplished several high frequency fatigue tests, of which range of the operation frequency is 5 Hz to 2500 Hz.

Main parameters of the excitation system are listed in Table 1, which are the same as those adopted in the theoretical simulation.

TABLE 1. Main parameters.

Parameters	Value
Rod side area of piston (A_r)	7.7×10^{-3} m^2
Head side area of piston (A_h)	1.54×10^{-2} m^2
Discharge coefficient (C_d)	0.62
Diameter of the spool (d)	1.6×10^{-2} m
Effective bulk modulus (E_h)	7.0×10^{8} Pa
Length of cylinder (L)	0.2 m
Mass of piston and load referred to piston (m)	6 kg
System pressure (p_s)	0.7×10^{7} Pa
Axial displacement of spool (x_v)	4×10^{-3} m
Density of oil (ρ)	900 kg/ m^3

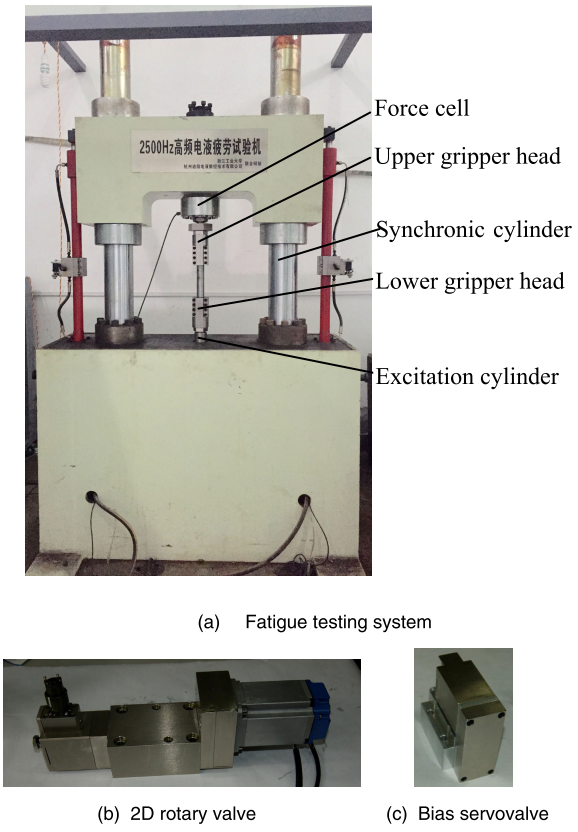

FIGURE 9. Prototype of the variable resonant electro-hydraulic fatigue testing system.

B. THEORETICAL AND EXPERIMENTAL RESULTS

Theoretical and experimental excitation waveforms are illustrated in Fig.10. Fig.10 (a) gives excitation waveforms in low frequency domain. It is noteworthy that the curve labeled as $x_v/x_{v0} = 1.0$ is a critical excitation waveform. Here, x_{v0} is defined as a threshold of the spool displacement with the conditions of the extreme excitation displacement ($y_p = p_s A_r/K_L$) and half a cycle ($\theta = 2\alpha$). The axial displacement of the spool is closer to the threshold, the excitation amplitude is larger until x_v is greater than x_{v0}. Once x_v is beyond x_{v0}, the system reaches pressure (displacement) saturation. As axial opening of the spool increases, the amplitude does not change, whereas the width of the peak (or saturated) 'platform' is broadened, resulting in a more rectangular shape of the waveform. Excitation waveforms in the mid frequency domain are shown in Fig.10 (b), these waveforms fairly approximate to sinusoidal waves. While displacement waves in high frequency region as shown in Fig.10 (c), the ascent and descent slopes show some deviations. Here, resonance is a factor that has to be considered in nearly all high frequency hydraulic system. While operated in the mid/high frequency domain, the excitation amplitude becomes extremely small and is almost not regulated by the spool displacement. Under these circumstances, the excitation action is not conspicuous in the experiment.

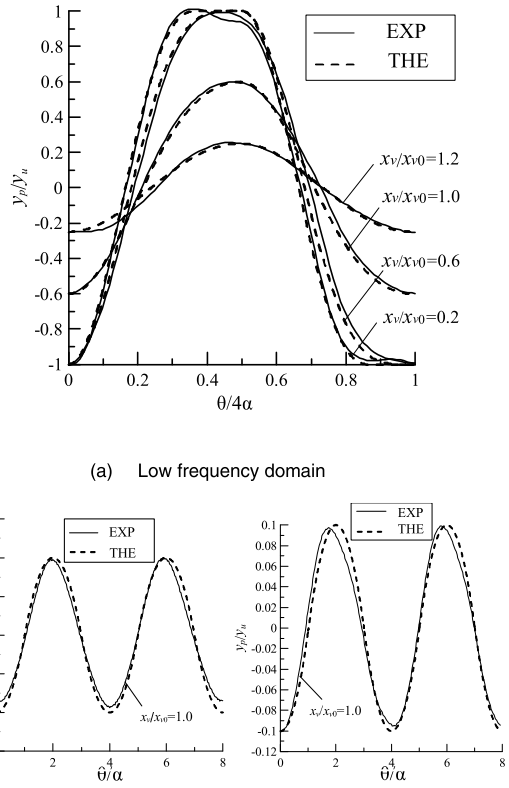

FIGURE 10. Theoretical and experimental excitation waveforms.

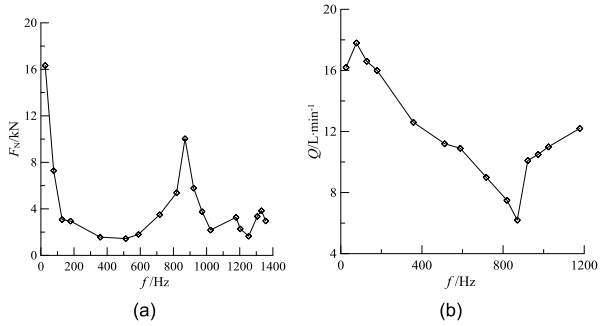

FIGURE 11. Characteristics of output force and flow for the initial length of the head chamber yp0=10 mm: (a) Output force versus excitation frequency; (b) Flow versus excitation frequency.

The excitation force and flow rate varies with the excitation frequency, as illustrated in Fig.11 to 13. At resonance, the output excitation force increases considerably and the flow rate is the minimum compared with other frequencies (initial lengths of the head chamber of the cylinder are different corresponding to these figures). Taken Fig.11 as an example, the system is capable of reaching an excitation force of 10 kN at resonant frequency 900 Hz in terms of the initial length of the head chamber is 10 mm. Therefore, the resonant excitation is believed to be an energy-saving excitation.

The fatigue testing system is vertical, so the gravity of the reciprocating motion unit is required to be overcome to complete the excitation. The central position of the vibration,

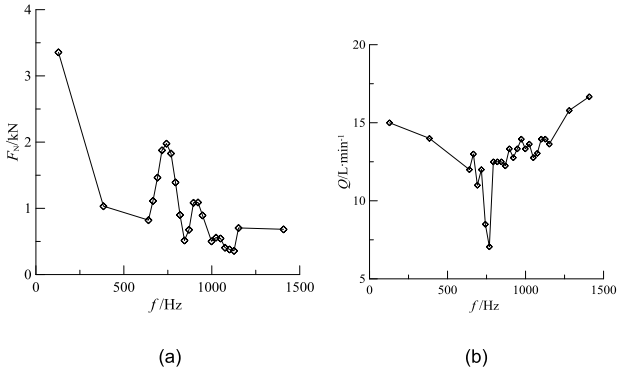

FIGURE 12. Characteristics of output force and flow for the initial length of the head chamber yp0=95mm: (a) Output force versus excitation frequency; (b) Flow versus excitation frequency.

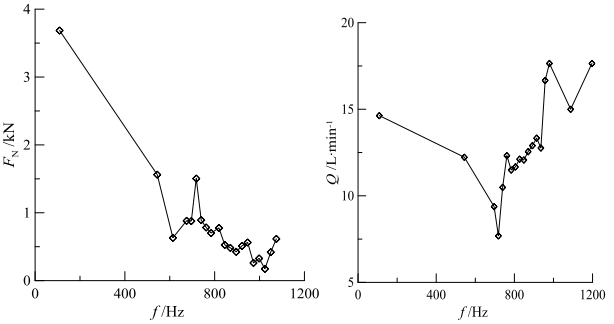

FIGURE 13. Characteristics of output force and flow for the initial length of the head chamber yp0=145mm: (a) Output force versus excitation frequency; (b) Flow versus excitation frequency.

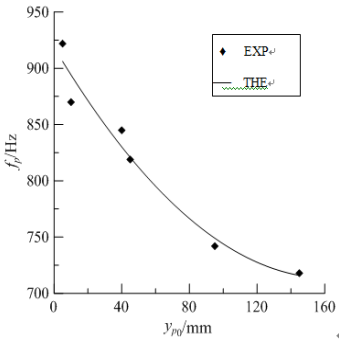

FIGURE 14. Resonant frequency versus initial head chamber volume of the cylinder.

as well as the initial volume of the head chamber of the cylinder, is controlled by the bias servovalve paralleled with 2D rotary valve to prevent the gravity (mainly including total mass of piston and load referred to piston). The position of the piston is obtained by a displacement transducer mounted inside the piston rod of the cylinder (high frequency excitation waveform is measured by force cell). Therefore, the initial position of excitation cylinder can be controlled accurately. As a result, the relationship between the over-all natural frequency of the excitation system and initial length of the head chamber of the cylinder is obtained, as shown in Fig.14. The actual setup provides minimum resonant

frequency of 720 Hz and a maximum of 924 Hz. The resonant frequency could be adjusted to satisfy the application requirements of different testing samples.

VII. CONCLUSION

A variable resonant electro-hydraulic fatigue testing system is designed, modeled and verified. The excitation waveforms of the system are derived analytically and verified experimentally with different loads in different frequency domains. The coupling relationship between the excitation amplitude and frequency are described analytically, including non-resonant and resonant mode. The prototype of the electro-hydraulic fatigue testing system is capable of being operated at 2500 Hz, thus it is not difficulty to be working in the resonant frequency (minimum resonant frequency of 720 Hz and a maximum of 924 Hz). Once at resonance, the excitation amplitude can be increased considerably and maintained at a high level, whereas the flow rate reaches the minimum value. The results indicate two unique features of the system, a suddenly increased excitation force and a small flow rate which is an energy-saving excitation at resonance relative to those at other frequencies. More specifically, the resonant frequency of this exciter could be regulated as the loads of the excitation system through the improved three-way valve-piston combination. These results and findings provide clear guidance for the understanding and designing of the electro-hydraulic excitation device, which will further broaden the application of the high frequency electro-hydraulic excitation method herein presented.

APPENDIX

$A_{vi}(\theta)$	instantaneous orifice areas on shoulder I ($i = 1$) or II ($i = 2$) of the spool (m^2)
A_h	head side area of piston (m^2)
A_r	rod side area of piston with $A_h = 2A_r$ (m^2)
A_{fl}	amplitude of the excitation in the low frequency domain (m)
A_{fm}	excitation amplitude in the mid frequency domain (m)
A_{fh}	excitation amplitude in the high frequency domain (m)
A_{rf}	resonant peak of the displacement waveform (m)
B_p	viscous damping coefficient (N/(m/s))
C_d	discharge coefficient
E_h	effective bulk modulus of system (Pa)
F_L	constant or arbitrary load force on piston (N)
K_L	load spring gradient (N/m)
K_v	flow gain
M_a	total mass of piston and load referred to piston (kg)
p_c	control pressure in head chamber (MPa)
p_{rc}	pressure in the control chamber at resonance (MPa)
p_{rL}	load pressure (MPa)
$p_{rL\max}$	amplitude of the pressure drop across the load at resonance (MPa)
Q_L	flow through the 2D rotary valve orifices (m^3/s)
r	radius of the spool (m)
V_0	initial head chamber volume (m^3)
w	a pressure ratio
x_v	axial displacement of spool (m)
y_v	peripheral width of the window overlapped by the groove on the spool (m)
y_p	displacement of piston (m)
y_{p0}	initial length of the head chamber (m)
y_l	negative end position of the excitation (m)
y_u	an extreme value as the control pressure could reach system pressure (m)
y_r	positive end position of the excitation (m)
y_{rp}	resonant displacement (m)
z	number of grooves on a single shoulder
α	central angle of every window (rad)
θ	angle coordinates with $\theta\omega_v t$

REFERENCES

[1] T. J. George, J. Seidt, and M. H. H. Shen, "Development of a novel vibration-based fatigue testing methodology," *Int. J. Fatigue*, vol. 26, no. 5, pp. 477–486, May 2004.
[2] S. E. Stanzl-Tschegg, "Very high cycle fatigue measuring techniques," *Int. J. Fatigue*, vol. 60, pp. 2–17, Mar. 2014.
[3] U. Karr, R. Schuller, and M. Fitzka, "Very high cycle fatigue testing of concrete using ultrasonic cycling," *Mater. Test.*, vol. 59, no. 5, pp. 438–444, May 2017.
[4] I. Hostens, J. Anthonis, and H. Ramon, "New design for a 6 DOF vibration simulator with improved reliability and performance," *Mech. Syst. Signal Process.*, vol. 19, no. 1, pp. 105–122, Jan. 2005.
[5] J. L. Xuan and S. K. Wang, "Development of hydraulic driven fatigue testing machine for insulators," *IEEE Access*, vol. 6, pp. 980–988, Nov. 2018.
[6] C. Ghielmetti, R. Ghelichi, and F. Guagliano, "Development of a fatigue test machine for high frequency applications," *Procedia Eng.*, vol. 10, pp. 2892–2897, May 2011.
[7] I. Milošević, P. Renhart, and G. Winter, "A new high frequency testing method for steels under tension/compression loading in the VHCF regime," *Int. J. Fatigue*, vol. 104, pp. 150–157, Nov. 2017.
[8] S. J. Cai, "Hydraulic ultra high frequency vibratory hammer," *Construct. Mach.*, vol. 1, pp. 6–8, Nov. 1995.
[9] W. M. Zhao, H. Y. Zu, and H. H. Lu, "Research of the hydraulic vibrating screen with the frequency modulation turn round valve for steplessly adjustable frequency," *Construct. Mach.*, vol. 3, pp. 83–86, Jul. 2005.
[10] Y. Ren and J. Ruan, "Regulating characteristics of an electro-hydraulic vibrator vibrator multiply controlled by the combination of a two-dimensional valve and a standard servo valve," *Proc. Inst. Mech. Eng., C, J. Mech. Eng. Sci.*, vol. 227, no. 12, pp. 2707–2723, Dec. 2013.
[11] J. Cui, F. Ding, and Q. P. Li, "Novel bidirectional rotary proportional actuator for electrohydraulic rotary valves," *IEEE Trans. Magn.*, vol. 43, no. 7, pp. 3254–3258, Jul. 2007.
[12] H. C. Tu, M. B. Rannow, and M. Wang, "Design, modeling, and validation of a high-speed rotary pluse-width-modulation on/off hydraulic valve," *ASME J. Dyn. Syst., Meas. Control*, vol. 134, no. 6, pp. 1–12, 2012.
[13] M. Pournazeri and A. Khajepour, "Precise lift control in a new variable valve actuation system using discrete-time sliding mode control," *Mechanism Mach. Theory*, vol. 99, pp. 217–235, May 2016.
[14] J. Ruan and R. T. Burton, "An electrohydraulic vibration exciter using a two-dimensional valve," *Proc. Inst. Mech. Eng., I, J. Syst. Control Eng.*, vol. 223, no. 2, pp. 135–147, Mar. 2009.
[15] T. Xing, X. W. Li, and H. J. Ma, "Study on resonance characteristics of hydraulic excited flutter device," *China Mech. Eng.*, vol. 25, pp. 1071–1074, Jul. 2014.
[16] J. M. Morgan and W. W. Milligan, "A 1 kHz servohydraulic fatigue testing system," in *Proc. Conf. High Cycle Fatigue Struct. Mater.*, Warrendale, PA, USA, 1997, pp. 305–312.

[17] G. Li, G. Shen, and Z. C. Zhu, "Sine phase compensation combining an amplitude phase controller and a discrete feed-forward compensator for electro-hydraulic shaking tables," *Trans. Inst. Meas. Control*, vol. 40, no. 11, pp. 3377–3389, Jul. 2018.
[18] B. K. Thoen, "Sinusoidal signal amplitude and phase control for an adaptive feedback control system," European Patent 0 563 063, Aug. 1996.
[19] N. Satoh, "Frequency characteristics of electro-hydraulic vibrator," *J. UOEH*, vol. 24, no. 4, pp. 405–412, Dec. 2002.
[20] Y. Tang, Z. C. Zhu, and G. Shen, "Real time acceleration tracking of electro-hydraulic shake tables combining inverse compensation technique and neural-based adaptive controller," *IEEE Access*, vol. 5, pp. 23681–23694, 2017.
[21] J. J. Yao, D. T. Di, and G. L. Jiang, "Acceleration amplitude-phase regulation for electro-hydraulic servo shaking table based on LMS adaptive filtering algorithm," *Int. J. Control*, vol. 85, no. 10, pp. 1581–1592, 2012.
[22] G. Palli, S. Strano, and M. Terzo, "Sliding-mode observers for state and disturbance estimation in electro-hydraulic systems," *Control Eng. Pract.*, vol. 74, pp. 58–70, May 2018.
[23] A. Plummer, "A general co-ordinate transformation framework for multi-axis motion control with application in the testing industry," *Control Eng. Pract.*, vol. 18, no. 6, pp. 598–607, Jun. 2010.
[24] W. Wei, Z. D. Yang, and J. W. Han, "Internal force decoupling control of hyper-redundant shaking table based on stiffness matrix," in *Proc. 2nd Int. Conf. Appl. Mech. Mater.* Kuala Laumpur, Malaysia: Trans. Tech. Publications, 2014, pp. 115–120.
[25] Y. Tang, Z. C. Zhu, and G. Shen, "Investigation on acceleration performance improvement of electro-hydraulic shake tables using parametric feedforward compensator and functional link adaptive controller," *ISA Trans.*, vol. 83, pp. 209–303, Dec. 2018.
[26] G. J. Yun, A. B. M. Abdullah, and W. Binienda, "Development of a closed-loop high-cycle resonant fatigue testing system," *Exp. Mech.*, vol. 52, no. 3, pp. 275–288, Mar. 2012.
[27] S. Schneider, R. Herrmann, and S. Marx, "Development of a resonant fatigue testing facility for large-scale beams in bending," *Int. J. Fatigue*, vol. 113, pp. 171–183, Aug. 2018.
[28] J. Diederley, R. Herrmann, and S. Marx, "Fatigue tests on large scale concrete specimens using the resonant test principle," *Beton-und Stahlbetonbau*, vol. 113, no. 8, pp. 589–597, Aug. 2018.
[29] M. Idriss and A. Elmahi, "Linear and nonlinear resonant techniques for characterizing cyclic fatigue damage in composite laminate," *Compos. B, Eng.*, vol. 142, pp. 36–46, Jun. 2018.
[30] I. Ursu, F. Ursu, and F. Popescu, "Backstepping design for controlling electrohydraulic servos," *J. Franklin Inst.-Eng. Appl. Math.*, vol. 343, no. 1, pp. 94–110, Jan. 2006.

YAN REN was born in 1980. She received the Ph.D. degree in mechanical engineering from the Zhejiang University of Technology, China, in 2011. She did her a Postdoctoral Research at the Zhejiang University of Technology, from 2012 to 2013. She is currently an Assistant Professor with Wenzhou University, China. Her research interests include electro-hydraulic digital control technology, components design, system design, and theoretical research.

JIPING BAI was born in 1976. He received the Ph.D. degree in mechanical engineering from the Zhejiang University of Technology, China, in 2014. He did his Ph.D. Research at the Zhejiang University of Technology, from 2007 to 2013. He is currently a Professor with the Zhejiang Institute of Communications, China. His research interests include electro-hydraulic digital control technology, components design, system design, and theoretical research.

JIAN RUAN was born in 1963. He received the Ph.D. degree from the School of Mechatronics Engineering, Harbin Institute of Technology, China, in 1989. He is currently a Professor with the Zhejiang University of Technology, China. His research interests include electro-hydraulic digital control components and control systems, electro-hydraulic vibration, pneumatic servo control, and nonlinear control theory and applications.